Analysis of temozolomide resistance in low-grade gliomas using a mechanistic mathematical model

Edouard Ollier, Pauline Mazzocco, Damien Ricard, Gentian Kaloshi, Ahmed Idbaih, Agusti Alentorn, Dimitri Psimaras, Jérôme Honnorat, Jean-Yves Delattre, Emmanuel Grenier, et al.

Received Date : 16-Sep-2016
Revised Date : 16-Nov-2016
Accepted Date : 23-Nov-2016
Article type : Original Article

Analysis of temozolomide resistance in low-grade gliomas by using a mechanistic mathematical model

Running title: Resistance to temozolomide in low-grade gliomas

Edouard OLLIER [a,b,c,#,*], Pauline MAZZOCCO [a,#], Damien RICARD [d,e], Gentian KALOSHI [f,g,h], Ahmed IDBAIH [f,g,h], Agusti ALENTORN [f,g,h], Dimitri PSIMARAS [f,g,h], Jérôme HONNORAT [i,j,k], Jean-Yves DELATTRE [f,g,h], Emmanuel GRENIER [a], François DUCRAY [i,j,l,#], Adeline SAMSON [c,#]

[#] Joint first authors and joint supervising authors.

[a] U.M.P.A., Ecole Normale Supérieure de Lyon, CNRS UMR 5669; INRIA, Project-team NUMED. 46 Allée d'Italie, 69364 Lyon Cedex 07, France

[b] SAINBIOSE, INSERM, U1059, Saint-Etienne, F-42023, FRANCE

[c] Université Grenoble-Alpes, Laboratoire Jean Kuntzmann, UMR CNRS 5224

[d] Service de Neurologie, Hôpital d'Instruction des Armées du Val-de-Grâce, Service de Santé des Armées, Paris, France

[e] UMR 5782 MD4 Cognac-G, CNRS, Service de Santé des Armées, Université Paris-

Descartes, Paris, France

[f] INSERM U975, Paris, France

[g] CNRS, UMR 7225, Paris, France

[h] AP-HP, Groupe Hospitalier Pitié-Salpêtrière, Service de neurologie 2-Mazarin, Paris, France.

[i] Hospices Civils de Lyon, Hôpital Neurologique, Service de Neuro-oncologie, Lyon, France

[j] Université Claude Bernard Lyon 1, Lyon, France

[k] Institut NeuroMyoGene (INMG) INSERM 1217 / UMR CNRS 5310, Lyon, France

[l] Cancer Research Centre of Lyon, INSERM U1052, CNRS UMR5286, Lyon, France

***CORRESPONDING AUTHOR**

Edouard Ollier

ENS de Lyon, UMPA UMR 5659 CNRS, 46 allée d'Italie, 69364 Lyon Cedex 07, FRANCE

Tel: +33 (0)4 72 72 84 44

E-mail: edouard.ollier@ens-lyon.fr

ABSTRACT

Understanding how tumours develop resistance to chemotherapy is a major issue in oncology. When treated with temozolomide (TMZ), an oral alkylating chemotherapy drug, most low-grade gliomas (LGG) show an initial volume decrease but this effect is rarely long lasting. In addition, it has been suggested that TMZ may drive tumour progression in a subset of patients as a result of acquired resistance. Using longitudinal tumour size measurements from 121 patients, the aim of the present study was to develop a semi-mechanistic mathematical model to determine whether resistance of LGG to TMZ was more likely to

result from primary and/or from chemotherapy-induced acquired resistance that may contribute to tumour progression. We applied the model to a series of patients treated upfront with TMZ (n = 109) or PCV (procarbazine, CCNU, vincristine) chemotherapy (n=12) and used a population mixture approach to classify patients according to the mechanism of resistance most likely to explain individual tumour growth dynamics. Our modelling results predicted acquired resistance in 51 % of LGG treated with TMZ. In agreement with the different biological effects of nitroso-ureas, none of the patients treated with PCV were classified in the acquired resistance group. Consistent with the mutational analysis of recurrent LGG, analysis of growth dynamics using mathematical modelling suggested that in a subset of patients, TMZ might paradoxically contribute to tumour progression as a result of chemotherapy-induced resistance. Identification of patients at risk of developing acquired resistance is warranted to better define the role of TMZ in LGG.

KEYWORDS: Low-Grade Glioma, Temozolomide, Resistance, Tumor Growth Inhibition, Mathematical Model.

INTRODUCTION

Adults' diffuse low-grade glioma (LGG) is a primary brain tumour. LGGs account for about 25% of gliomas and are characterized radiologically by slow and continuous growth preceding anaplastic transformation [1]. However, despite surgery, radiotherapy and chemotherapy, most tumours recur and remain incurable with a median survival of 5 to 15 years. Among chemotherapeutic treatments, temozolomide (TMZ), an alkylating agent, has improved the prognosis of glioblastomas, especially in tumours that have a methylated MGMT promoter and therefore cannot repair TMZ-induced DNA damages [2]. In LGG, however, despite the presence of a methylated MGMT promoter in most patients, the benefit of TMZ remains unclear [3]. Growth kinetic studies have shown that TMZ most frequently

results in an initial volume decrease but that this effect is rarely long lasting with most patients developing tumour progression either during or shortly after TMZ disruption [4]. In addition, mutational analyses in recurrent LGG have demonstrated that, in a subset of patients, TMZ leads to the acquisition of a hypermutation phenotype which is associated with increased mitotic activity and could contribute to malignant progression through mutations in the RB and AKT-mTOR pathways [5]. This phenomenon is thought to result from inactivating mutations of the DNA mismatch repair (MMR) pathway which has been shown to be a mechanism of acquired resistance to TMZ, especially in gliomas with a methylated MGMT promoter [6-10]. Therefore, in a subset of LGG, the mutagenic effect of TMZ could induce inactivating mutations in MMR genes resulting in acquired resistance to TMZ and in a detrimental hypermutation phenotype as a result of continued TMZ exposure [6].

Mechanisms of LGG resistance to TMZ remain unclear, although we can suppose that two types of resistance exist: i) primary resistance and ii) acquired resistance. Primary resistance may correspond to natural tumour capacity to resist to treatment damages, such as p53 mutation and MGMT hypermethylation. As for acquired resistance, it corresponds to genetic and epigenetic changes in neoplastic cells initially sensitive to treatment. Acquired resistance arises with TMZ treatment, and can be linked to MGMT production increase [11], or to new mutations appearing after TMZ onset [5, 7]. Nevertheless, these hyper mutated recurrent cancer cells are not observed in all patients treated with TMZ, and there is currently no available pre-TMZ treatment biomarker that can help to prevent this emergence of resistance. Understanding how LGG develop resistance to treatment is therefore a major issue.

Our aim herein is to propose a semi-mechanistic model, describing the different processes of emergence of resistance for LGG treated with TMZ. In this view, our mathematical model distinguishes between sensitive cells, primary resistant cells and cells becoming resistant due to exposure to treatment. We furthermore present a statistical population mixture model that

allows to determine if a given patient developed acquired resistance or not. Associations between predicted resistance profiles, LGG molecular characteristics and outcome are then studied. In order to explore whether the resistance profile might be different in patients treated with PCV chemotherapy (Procarbazine, CCNU, Vincristine), another chemotherapy regimen used in LGG, a subset of patients who received this treatment is also analysed.

MATERIAL AND METHODS

Data

We analysed longitudinal follow-up of tumour size measurements in 121 patients treated with upfront chemotherapy (109 patients with TMZ, 12 patients with PCV) and in whom time-course of tumour size was available before, during and after treatment [12]. Tumour sizes were expressed as mean tumour diameters (MTD) estimated from magnetic resonance imaging (MRI) [12]. MRIs were performed every 4 to 6 months before and after treatment. During the treatment, MRIs were performed every 3 months. For each patient, 12 MRI were performed on averaged, with at least 2 MRI before treatment onset and 4 after. One TMZ cycle corresponds to a daily administration of 200 mg/m^2 of TMZ for five consecutive days. Patients included in the study received one cycle of TMZ per month for up to two years. PCV administration protocol consists of up to 6 cycles, with intervals of 6 weeks between cycles: CCNU (110 mg/m^2) administered on day 1, procarbazine (60 mg/m^2) administered on days 8 to 21, and vincristine (1.4 mg/m^2, max. 2 mg) administered on days 8 and 29.

In most patients, TMZ resulted in an initial reduction in tumour size, which was followed by tumour regrowth either during treatment or after TMZ administration. Figure 1 displays three different individual profiles that are observed in our population of patients treated with TMZ, where duration of treatment is represented with the grey shaded area. The left graph represents an example of a patient who experienced tumour progression during treatment. For

the two other patients, the tumour regrows immediately after treatment disruption (middle graph) and after a certain time (right graph). Note that no tumour regrowth during PCV treatment was observed, but rather a prolonged response for several months after cessation of treatment.

In addition to tumour size measurements, data on survival and genetic information were also available for patients treated with TMZ. Progression-free and overall survivals were computed as the time between treatment onset and clinical progression or death respectively. Patients lost to follow-up were censored at the time of last news. For 71 out of the 109 patients treated with TMZ, the following molecular characteristics were available: 1p/19q chromosomal co-deletion, p53 overexpression, and IDH mutation status. MGMT promoter methylation was available in 53 patients.

Mathematical models for resistance in low-grade gliomas treated with chemotherapy

We first developed two models describing each of them a different resistance profile. The first model, called model PR, describes LGG dynamics assuming there are only primary resistant cells. The second model, called model PAR, describes LGG dynamics assuming both primary and acquired resistant cells are present in the tumour. These two models are schematically represented in Figure 2.

For model PR, we assume that the tumour is initially composed of sensitive cells, denoted S and primary resistant cells, denoted R_P. During treatment, chemotherapy induces DNA lesions to sensitive cells only. They then become damaged cells (denoted D) with a rate $\tau_{SD}C(t)$, where $C(t)$ is the chemotherapy blood concentration. Damaged cells eventually die with a rate μ_D. We assume that sensitive and primary resistant cells proliferate with the same growth rate λ. Mathematical formulation of this model is as follows:

$$\begin{cases} \dfrac{dS}{dt} = \lambda \times S \times \left(1 - \dfrac{P^{PR}}{120}\right) - \tau_{SD} \times C(t) \times S & with \quad S(0) = k_s \times P_0 \\ \dfrac{dD}{dt} = \tau_{SD} \times C(t) \times S - \mu_D \times D & with \quad D(0) = 0 \\ \dfrac{dR_P}{dt} = \lambda \times R_P \times \left(1 - \dfrac{P^{PR}}{120}\right) & with \quad R_P(0) = (1 - k_S) \times P_0 \end{cases} \qquad (A)$$

where $P^{PR} = S + D + R_P$ is the total tumour size, P_0 is the initial mean tumour diameter and k_S represents the initial proportion of sensitive cells in the tumour. The tumour is assumed to grow according to a logistic model with maximal tumour size fixed to 120 mm, a choice consistent with the maximal tumour size observed in clinical practice [4].

For TMZ, blood concentration C is supposed to follow a mono-compartmental kinetic [13]:

$$C(t) = \sum_{d=1}^{N_D} \frac{D \times k_a}{V \times k_a - Cl} \left(e^{-\frac{Cl}{V}(t-t_d)_+} - e^{-k_a (t-t_d)_+} \right)$$

where k_a, Cl, and V are, respectively, the absorption coefficient, the clearance, and the volume of distribution of TMZ. Other ways to implement TMZ concentration would have been possible. For example, the TMZ concentration could have been supposed to be constant during the treatment period. However, this hypothesis seemed to us less realistic than to use a previously published PK model to simulate TMZ concentrations. In addition assuming a continuous TMZ concentration may have introduced a bias in parameters estimate. For PCV, we did not model the three drugs separately. Following the work of Ribba et al. [14], we defined PCV's concentration $C(t)$ as a unique variable representing a virtual drug administrated intravenously at a dose D fixed to 1:

$$C(t) = \sum_{d=1}^{N_D} (t - t_d)_+ \times e^{-k_e (t-t_d)_+}$$

where k_e is the rate of decay of PCV concentration.

For model PAR, we assumed that resistant cells emerge due to exposure to chemotherapy, in addition to pre-existing resistant cells. As in model PR, the tumour is initially composed of sensitive cells S and primary resistant cells R_P, only sensitive cells being affected by the treatment. However, in this model, damaged cells D can either die with a rate μ or become resistant with a rate τ_{DR} due to new mutations for instance. These resistant cells, denoted R_A in the model, proliferate at a rate λ_R. Mathematical formulation is as follows:

$$\begin{cases} \dfrac{dS}{dt} = \lambda \times S \times \left(1 - \dfrac{P^{PAR}}{120}\right) - \tau_{SD} \times C(t) \times S & with \quad S(0) = k_s \times P_0 \\ \dfrac{dD}{dt} = \tau_{SD} \times C(t) \times S - \left(\tau_{DR_A} + \mu_D\right) \times D & with \quad D(0) = 0 \\ \dfrac{dR_A}{dt} = \lambda \times \left(1 + \Delta_{R_A}\right) \times R_A \times \left(1 - \dfrac{P^{PAR}}{120}\right) + \tau_{DR_A} \times D & with \quad R_A(0) = 0 \\ \dfrac{dR_P}{dt} = \lambda \times R_P \times \left(1 - \dfrac{P^{PAR}}{120}\right) & with \quad R_P(0) = \left(1 - k_S\right) \times P_0 \end{cases} \qquad (B)$$

where $P^{PAR} = S + D + R_P + R_A$ represents the total tumour size. Because TMZ can induce malignant transformation, and thus faster tumour growth [5], we further assumed that acquired resistant cells divide at a rate that could be greater than or equal to λ. Therefore we set $\lambda_R = \lambda(1+\Delta_R)$, with $\Delta \geq 0$. Blood concentration of chemotherapy is modelled as described above.

Population Mixture Model

As hypermutation phenotype was not clinically observed in all patients treated with TMZ, we could assume that tumours can, but do not necessarily develop acquired resistance. Instead of describing all patients with either model PR or model PAR, it could be interesting to determine which model is more suitable for a given patient. Resistance profile (PR or PAR)

is therefore viewed as an unknown status to determine, as we do not know *a priori* which resistance profile corresponds the best. We thus introduced a population mixture model, allowing to describe both profiles within the same framework, and to classify patients in one or the other resistance profile.

Let us denote by y_{ij} tumour measurement at time t_{ij} for the i-th patient and ϕ_i its individual parameters. We introduce a Between Subject Model Mixture (BSMM) describing tumour observations as follows [15]**:**

$$\begin{cases} y_{ij} = P^{PAR}(t_{ij},\phi_i) + \varepsilon_{ij} \quad with \quad \Pr(G^i = PAR) = \pi_{PAR} \\ y_{ij} = P^{PR}(t_{ij},\phi_i) + \varepsilon_{ij} \quad with \quad \Pr(G^i = PR) = 1 - \pi_{PAR} \end{cases} (C)$$

Where G_i is the resistance profile of patient i, P^{PR} and P^{PAR} are the tumour size obtained with models (A) and (B) respectively. Residual errors ε_{ij} are assumed to be normally distributed with mean equal to 0, and standard deviation equal to σ. To summarize equation (C), the BSMM assumes that the growth curve of each subject follows one of the two previously described models (PR or PAR) but without knowing which one a priori. The proportion of the population associated to each of the two models is unknown a priori. Each subject has a label G^i corresponding to the model from which it has been generated. This label is inferred using an estimation algorithm. This estimated label is the used to classify the subjects in the two groups. This mixture model enables to describe both patients with primary resistance only and patients who develop acquired resistance within the same model. Such statistical model has been successfully used to detect non-responder to a given treatment [15,16] or to describe complex absorption process [17]. Finally, the vector of individual parameters ϕ_i was given by $\phi_i = (\lambda_i, \Delta_i, \tau_{SD_i}, \tau_{DR_i}, \mu_{D_i}, k_{S_i}, P_{0_i})$. We assumed that all parameters were log-normally distributed, except k_S that was assumed to follow a logit-normal distribution.

Model Development and Evaluation

Model development was based on TMZ data set as the model's hypothesis are based on biological results obtained from patients treated with TMZ. During this first step, we determined which model structure best fitted the data between P^{PR}, P^{PAR}, or BSMM. Once a model's structure was selected, final estimates were obtained using TMZ and PCV data sets that had been pooled together to study potential differences between TMZ- and PCV-treated patients.

Population parameters were estimated using the SAEM algorithm [18] implemented in the Monolix software [19]. Model evaluation and selection were based on the visual inspection of the goodness of fit plots, precision of parameter estimates and a decrease in Bayesian Information Criterion (BIC). Shrinkage of individual random effects and residual error was also assessed [20]. The goodness of fit was established by plotting the population predictions of the model *vs.* observations, individual predictions *vs.* observations and visual predictive check. All graphics were generated using the package ggplot2 [21] with R software [22].

Analysis of Clusters' Characteristics for patients treated by TMZ

When considering the mixture model, each patient is assigned to a cluster. Patients' characteristics of both clusters are compared using a Student test for continuous variables and a chi-squared test for categorical ones. Progression-free survival (PFS) and overall survival (OS) are studied using the Kaplan-Meier method. Difference between PFS and OS in both clusters is assessed using a Log-Rank test. A multivariate survival analysis is conducted

using a Cox proportional hazard model to adjust for age, mutation status and tumour size at TMZ onset. Statistical significance of each variable is assessed using a Wald test.

RESULTS

Model development and evaluation

We first studied whether resistance to TMZ most likely results from primary resistance only (model PR) or from primary and acquired resistance (model PAR). For this purpose, we independently estimated parameters of models PR and PAR on the TMZ data set only. Parameter τ_{SD}, standing for the rate of transition from sensitive cells to damaged ones, was considered as fixed effect since it improved the quality of parameter estimates and had no impact on the goodness of fit plots. Moreover it prevents identifiably issues due to the lack of pharmacokinetic data. We found that model PAR performs better than model PR (BIC=7489 compared to 7670 with model PR), showing that taking into account the two types of resistance more accurately describes experimental data than taking into account primary resistance only.

However, because all tumours do not exhibit hyper mutation phenotype after TMZ treatment [5], and therefore may not develop acquired resistance, we investigated whether model PAR is suitable for all patients. For this purpose, we estimated parameters of the mixture model, which allows patients to be described either with model PR or with model PAR. This latter yielded to even better results suggesting that resistance to TMZ in LGG is variable, resulting from primary resistance only in some patients and from both (primary and acquired resistance) in others. The BSMM mixture model improved data fitting as demonstrated by the decrease of BIC value (BIC =7466 for BSMM), and led also to a more

accurate parameter estimates and a decrease of variances of random effects. Shrinkage values for parameters τ_{DR} and Δ_R remained high (between 45% and 60%), indicating an identifiably issue in individual random effects. In consequence, no inter-individual variability was allocated to these two parameters. It improved shrinkage values and precision of parameter estimates.

After having identified the BSMM model as the model that best fits data in LGG patients treated with upfront TMZ, we estimated parameters of the BSMM model using the whole dataset of patients (i.e including also patients treated with upfront PCV chemotherapy). Population parameter estimates (mean value and inter-individual variability) are presented in Table 1. Note that as Δ_R was estimated different to zero, it implies a faster proliferation of acquired resistant cells, which support the hypothesis of increased mitotic activity. All parameters were accurately estimated with residual standard errors smaller than 25%. Highest shrinkage value of individual random effects was 31%. Shrinkage value of residual errors was 14% indicating good identifiably of the proposed model. Individual parameters were then estimated. In the same time, the 121 patients were classified into one of the two clusters, according to the mechanism of resistance (primary resistance only or primary and acquired resistance) most likely to explain their individual tumour growth dynamics. Among patients treated with upfront TMZ, 56 patients (51%) were assigned to PAR cluster (primary and acquired resistance) and 53 patients (49%) to PR cluster. In contrast, all patients treated with upfront PCV were assigned to PR cluster.

Model validation was then performed using observed versus predicted plots and Visual Predictive Check (VPC). The are presented in Figure 3 and Figure 4. Concerning VPC plots in TMZ treated patients, left plot represents VPC for PR cluster, while right plot is VPC for PAR cluster. Data fall into confidence intervals for both clusters, indicating good properties of the population model. Tumour regrowth occurs sooner in the PAR cluster, and

tumour size increases faster after TMZ onset. For both cluster, the 95-th quantiles seem to over predict tumour re-growth. This phenomenon is partially due to missing information as a consequence of an informative censoring process. Indeed, the follow up of most patients ended quickly after tumour re-growth because of the initiation of a new therapeutic.

Figure 5 displays examples of individual fits for patients in each cluster, with dynamics of each sub-population of cells. As shown, the model is able to reproduce different patterns of growth dynamics in each cluster.

Impact of genetic mutations and survival analysis

There was no significant difference between baseline characteristics of patients clustered in PR or PAR profile, including age, tumour size at TMZ onset, sex, p53 expression, IDH mutation status, 1p/19q co-deletion status and MGMT methylation status.

However, their outcome was different (Figure 6). Patients with acquired resistance to TMZ have both a shorter median progression free survival (22.7 months (95\% CI = 16.0 to 28.6) versus 49 months (95\% CI = 37.9 to 57.2), p-value < 0.001) and a shorter median overall survival (50.7 months (95\% CI = 35.3 to 76.4) versus 139.5 months (95\% CI= 86.4 to not reached), p-value < 0.001) compared to patients without acquired resistance. This result is coherent with the model's assumption as acquired resistance enhance tumour growth. On multivariate analysis, the impact of acquired resistance to TMZ was independent of age, molecular profile (p53 overexpression, IDH mutation and 1p/19q co-deletion) and tumour size at TMZ onset (Table 2 and right plot in Figure 6).

DISCUSSION

It has been recently suggested that because of acquired resistance, TMZ may paradoxically drive tumour progression in LGG [5-6]. Consistently, in the present study, using mathematical modelling, we show that in a subset of LGG, tumour growth dynamics is best described by the hypothesis of a detrimental TMZ-induced resistance and that this phenomenon is associated with worst outcome independently of classical prognostic factor.

Resistance to treatments is one of the main causes of therapeutic failures in oncology. Mathematical modelling has been shown to be an effective strategy to investigate resistance mechanisms to chemotherapy and to propose new therapeutic strategies [23-24]. There is a long tradition of mathematical modelling of both resistance to chemotherapy and of glioma growth; however, to the best of our knowledge, no study has specifically focused on modelling resistance to chemotherapy in LGG. Most of the models that have been proposed to describe and analyse cancer resistance to chemotherapy have considered the tumour as being composed of two cell populations: one population of sensitive cells and one population of resistant cells. In the 1980s, [25] first proposed such a model based on ODE. This pioneering model effectively accounted for kinetic resistance in breast cancer treated with cell cycle phase-specific chemotherapy based on the distinction of sensitive/resistant and proliferative/quiescent cells. Thereafter, this framework was widely used to explore different hypotheses in cancer resistance such as optimal dosing schedules and the potential implications of cancer stem cells in drug resistance [23,26]. However, these models were not developed to explicitly differentiate primary from acquired resistance. For this purpose, Komarova et al [27] proposed a discrete space markov process; but, this model was not calibrated using clinical data, and may be computationally very demanding. Terranova et al [28] proposed an ODE model incorporating different resistant cell subpopulations allowing

the description of both primary and acquired resistance. Here again, the model was not calibrated using real data. Finally, in the specific context of LGG, Mazzocco et al [29] developed a tumour growth inhibition model of LGG treated with TMZ, in which parameters were estimated using longitudinal tumour size measurements. In this model, however, resistance to TMZ was described using an empirical parametric function, giving no insight on resistance mechanisms, as treatment efficacy was simply considered to decrease with time.

The aim of our study was to develop a model to investigate TMZ resistance in LGG. To our knowledge, this is the first study trying to classify patients according to their potential resistance mechanisms. For this purpose, we developed a model describing both primary and chemotherapy-induced resistance using a data-driven approach. We distinguished different cell subpopulations: sensitive cells, primary resistant cells, damaged cells, and cells that become resistant after being damaged. After evaluating different models, we found that, in agreement with the hypothesis of a detrimental TMZ-driven progression in a subset of patients, the model that most accurately described the data was a model considering that resistance to TMZ in LGG is heterogeneous, consisting of either primary resistance only or primary and acquired resistance contributing to tumour progression. A potential development of the model would be to use it to identify patients who may not benefit from TMZ. However, in the current version of the model, to accurately classify patients, we need observations during and after treatment with TMZ. In order to detect as early as possible patients who develop acquired resistance, or even to predict it, we would need to include covariates such as p53 mutation, IDH mutations or MGMT promoter hypermethylation in the model, particularly on parameter π_{PAR}. In the present study, however, these molecular characteristics were not available in every patients making impossible evaluation of these covariates according to a mixed model approach.

Due to the lack of patients who underwent re-resection after TMZ progression, we could not determine whether in recurrent tumours clustered with acquired resistance, features suggestive of acquired resistance such as MMR gene mutations or a hypermutation phenotype were found. However, our modelling results are supported by striking similarities with those of the mutational analysis performed in recurrent LGG after TMZ. These analyses have shown that the acquisition of a hypermutation profile after TMZ treatment was only observed in a subset of patients (6 out 10 LGG analyzed [5]), was associated with an increased mitotic activity, and occurred in both LGG with and without the 1p/19q co-deletion [5,30]. Consistently, our model predicted that acquired resistance to TMZ only occurred in a subset of patients (56 out of 109 patients), occurred independently of LGG molecular characteristics (especially 1p/19q co-deletion) and was associated with a much important growth rate during tumour progression. Our modelling results are also indirectly supported by the fact that none of the patients treated with PCV chemotherapy were classified into the acquired resistance cluster. Indeed, in contrast to TMZ, the effect of CCNU, which is a nitrosourea and the main drug of the PCV regimen, is not mediated by the MMR pathway. To our knowledge, the genomic profile of recurrent LGG after PCV chemotherapy has not been assessed; however, several in vitro studies have shown that in contrast to TMZ, an exposure to nitrosoureas does not lead to the acquisition of a hypermutation phenotype [31-33].

TMZ induced-hypermutation phenotype has been suggested to be detrimental but its clinical impact has not been studied yet. It would require the analysis of a large number of re-operated recurrent LGG. Owing to the absence of a biological validation, our model results must be taken with caution, although they suggest that TMZ-induced resistance may have a

negative clinical impact. Indeed, in our model, predicted acquired resistance was associated with shorter overall survival independently of age, tumour size, and of LGG molecular characteristics, namely 1p/19q co-deletion. This finding may have important clinical consequences. In recent years, upfront chemotherapy with TMZ has been developed as a strategy to defer radiotherapy and its potential neurotoxicity in LGG patients. The preliminary results of a randomized phase III study comparing initial TMZ versus initial RT suggested that this strategy might be effective in 1p/19q co-deleted but not in LGG without 1p/19q co-deletion [34]. Yet, our modelling results suggest that even in 1p/19q co-deleted LGG, TMZ might be detrimental in patients at risk of developing acquired resistance.

Although our modelling results provide original insight into the resistance mechanism of LGG after chemotherapy, some points will need to be further investigated. The lack of validation of our prediction is the principal limitation of this work. The validation of our predictions will need: i) to validate at the biological level that our patients with acquired resistance have a hyper mutated phenotype and ii) to validate our model in an external dataset. The association with the worst outcome will also need to be validated in an independent study. Nevertheless, together with mutational analysis of recurrent LGG after TMZ, our study suggests that beyond LGG current molecular classification, the benefit of TMZ may depend on the tumour capacity to develop acquired resistance and that identification of patients at risk of developing acquired resistance will be important to better define the role of TMZ in LGG.

CONFLICT OF INTEREST

The authors disclose no potential conflicts of interest.

ACKNOWLEDGEMENTS

We thank Marie-Aline Renard, Yannick Marie and Blandine Boisselier for excellent technical assistance. This work has been partially supported by the LabEx PERSYVAL-Lab (ANR-11-LABX-0025-01) funded by the French program Investissement d'avenir.

REFERENCES

1. Ricard D., Idbaih A., Ducray F., Lahutte M., Hoang-Xuan K., Delattre J.Y. Primary brain tumours in adults. The Lancet (2012) **379** 1984-1996.
2. Hegi M.E., Diserens A.C., Gorlia T., Hamou M.F., de Tribolet N., Weller M. et al. MGMT gene silencing and benefit from temozolomide in glioblastoma. New England Journal of Medicine. (2005) 352 997-1003.
3. van den Bent M.J. Chemotherapy for low-grade glioma: when, for whom, which regimen? Current Opinion in Neurology. (2015) **28** 633-938.
4. Ricard D., Kaloshi G., Amiel-Benouaich A., Lejeune J., Marie Y., Mandonnet E. et al. Dynamic history of low-grade gliomas before and after temozolomide treatment. Annals of Neurology. (2007) **61** 484-90.
5. Johnson B.E., Mazor T., Hong C., Barnes M., Aihara K., McLean C.Y. et al. Mutational analysis reveals the origin and therapy-driven evolution of recurrent glioma. Science. (2014) **343** 189-193.
6. Thuijl H.F. Van, Mazor T., Johnson B.E., Fouse S.D., Aihara K., Hong C. et al. Evolution of DNA repair defects during malignant progression of low □ grade gliomas

after temozolomide treatment. Acta Neuropathol. (2015) **129** 597-607.

7. Yip S., Miao J., Cahill D.P., Iafrate A.J., Aldape K., Nutt C.L. et al. MSH6 mutations arise in glioblastomas during temozolomide therapy and mediate temozolomide resistance. Clinical Cancer Research. (2009) **15** 4622-4629.
8. McLendon R., Friedman A., Bigner D., Van Meir E.G., Brat D.J., Mastrogianakis G.M. et al. Comprehensive genomic characterization defines human glioblastoma genes and core pathways. Nature (2008) **455** 1061-1068.
9. Hunter C., Smith R., Cahill D.P., Stephens P., Stevens C., Teague J. et al. A hypermutation phenotype and somatic MSH6 mutations in recurrent human malignant gliomas after alkylator chemotherapy. Cancer Research. (2006) **66** 3987-3991.
10. Cahill D.P., Levine K.K., Betensky R.A., Codd P.J., Romany C.A., Reavie L.B. et al. Loss of the mismatch repair protein MSH6 in human glioblastomas is associated with tumour progression during temozolomide treatment. Clinical Cancer Research. (2007) **13** 2038-2045.
11. Kitange G. J., Carlson B. L., Schroeder M. A., Grogan P. T., Lamont J. D., Decker P.A., Wu W., James C. D., Sarkaria J. N. Induction of MGMT expression is associated with temozolomide resistance in glioblastoma xenografts. Neuro-oncology. (2009) **11** 281–291.
12. Kaloshi G., Benouaich-Amiel A., Diakite F., Taillibert S., Lejeune J., Laigle-Donadey F. et al. Temozolomide for low-grade gliomas: Predictive impact of 1p/19q loss on response and outcome. Neurology. (2007) **68** 1831-1836.
13. Ostermann S., Csajka C., Buclin T., Leyvraz S., Lejeune F., Decosterd L. et al. Plasma and cerebrospinal fluid population pharmacokinetics of temozolomide in malignant glioma patients. Clinical Cancer Research. (2004) **10** 3728-3736.
14. Ribba B., Kaloshi G., Peyre M., Ricard D., Calvez V., Tod M. et al. Pallud. A tumour

growth inhibition model for low-grade glioma treated with chemotherapy or radiotherapy. Clinical Cancer Research. (2012) **18** 5071-5080.

15. Mbogning C., Bleakley K., Lavielle M. Between-subject and within-subject model mixtures for classifying hiv treatment response. Prog. Appl. Math. (2012) **4** 148-166.

16 Shiiki T., Hashimoto Y., Inui K.I. Simulation for population pharmacodynamic analysis of dose-ranging trials: usefulness of the mixture model analysis for detecting nonresponders. Pharmaceutical reashearch. (2002) **19** 909-913.

17. Ollier E., Hodin S., Basset T., Accassat S., Bertoletti L., Mismetti P., Delavenne X. In vitro and in vivo evaluation of drug-drug interaction between dabigatran and proton pump inhibitors. Fundam. Clin. Pharmacol. (2015) **29** 604–614.

18. Lavielle M., Mbogning C. An improved SAEM algorithm for maximum likelihood estimation in mixtures of non linear mixed effects models. Stat. Comput. (2014) **24** 693-707.

19. Lixoft-Incuballiance. Monolix User Guide Version 4.3.3. 2014; Available from: http://www.lixoft.eu/wp-content/uploads/2015/06/UsersGuide.pdf

20. Savic R.M., Karlsson M.O. Importance of shrinkage in empirical bayes estimates for diagnostics: problems and solutions. The AAPS Journal. (2009) **11** 558-569.

21. Wickham H. ggplot2: elegant graphics for data analysis. Springer. 2009;

22. R Development Core Team. R: A language and environment for statistical computing. R Foundation for Statistical Computing, Vienne, Austria, 2012. ISBN 3-900051-07-0. 2014; Available from: http://www.r-project.org

23. Sostelly A., Payen L., Guitton J., Di Pietro A., Falson P., Honorat M., Boumendjel A., Gèze A., Freyer G., Tod M. Quantitative evaluation of the combination between cytotoxic drug and efflux transporter inhibitors based on a tumour growth inhibition model. Fundam. Clin. Pharmacol. (2014) **28** 161-169.

24. Foo J., Chmielecki J., Pao W., Michor F. Effects of pharmacokinetic processes and varied dosing schedules on the dynamics of acquired resistance to erlotinib in egfr-mutant lung cancer. J. Thorac. Oncol. (2012) **7** 1583-1593.

25. Birkhead B., Rankin E., Gallivan S., Dones L., Rubens R. A mathematical model of the development of drug resistance to cancer chemotherapy. Eur. J. Cancer Clin. Oncol. (1987) **23** 1421-1427.

26. Tomasetti C., Levy D. Role of symmetric and asymmetric division of stem cells in developing drug resistance. Proceedings of the National Academy of Sciences. (2010) **107** 16766-16771.

27. Komarova N. Stochastic modeling of drug resistance in cancer. J. Theor. Biol. (2006) **239** 351-366.

28. Terranova N., Girard P., Klinkhardt U., Munafo A. Resistance development : a major piece in the jigsaw puzzle of tumour size modeling. CPT. (2015) **4** 320-323.

29. Mazzocco P., Barthélémy C., Kaloshi G., Lavielle M., Ricard D., Idbaih A. et al. Prediction of response to temozolomide in low-grade glioma patients based on tumour size dynamics and genetic characteristics. CPT: Pharmacometrics Syst Pharmacol. (2015) **4** 728-737.

30. Mazor T., Johnson B.E., Grimmer M., Hong C., Hamilton E.G., Jones E.L., et al. Hypermutation and malignant progression in an expanded cohort of temozolomide-treated low-grade glioma patients. Neuro Oncol. (2015) **17 (suppl. 5)** 97-97.

31. Takagi Y., Hidaka M., Sanada M., Yoshida H., Sekiguchi M. Different initial steps of apoptosis induced by two types of antineoplastic drugs. Biochemical Pharmacology. (2008) **76** 303-311.

32. Sanada M., Hidaka M., Takagi Y., Takano T.Y., Nakatsu Y., Tsuzuki T., et al. Modes of actions of two types of anti-neoplastic drugs, dacarbazine and ACNU, to induce apoptosis. Carcinogenesis. (2007) **28** 2657-2663.

33. Bodell W.J., Gaikwad N.W., Miller D., Berger M.S. Formation of DNA adducts and induction of lacI mutations in big blue rat-2 cells treated with temozolomide implications for the treatment of low-grade adult and pediatric brain tumours. Cancer Epidemiology Biomarkers & Prevention. (2003) **12** 545-551.

34. van den Bent M.J. Chemotherapy for low-grade glioma: when, for whom, which regimen? Current opinion in neurology. (2015) **28** 633–938.

Table 1: Estimated values of the population parameter

	Population mean (% RSE)	**Inter-patient variability (% RSE)**	**Shrinkage (%)**
Tumor Growth Parameters			
λ (d^{-1})	0.000385 (8)	0.745 (9)	0.16
Δ_{R_A}	11 (11)	-	-
τ_{SD}($L.g^{-1}.d^{-1}$)	0.0382 (10)	-	-
τ_{DR} (d^{-1})	0.000544 (24)	-	-
μ_D (d^{-1})	0.00219 (9)	0.701 (10)	0.27
k_S	0.474 (5)	0.65 (10)	0.31
P_0 (mm)	40 (5)	0.503 (7)	0.01
Pharmacokinetic Parameters of TMZ			
k_a (d^{-1})	140 (fixed)	-	-
V (L)	30 (fixed)	-	-
Cl ($L.d^{-1}$)	240 (fixed)	-	-

Pharmacokinetic Parameters of PCV			
k_e	0.025 (fixed)	-	-
Mixture Parameter			
π_{PAR}	0.48 (13)	-	-
Residual Error Parameter			
σ	2.31 (2)	-	0.14

λ: division rate of sensitive and primary resistant cells, Δ_{R_A}: increase in division rate of acquired resistant cells, τ_{SD}: transition rate from sensitive to damaged cells, τ_{DR}: transition rate from damaged to acquired resistant cells, μ_D: death rate of damaged cells, k_S: proportion of sensitive cells at the beginning of the follow-up, P_0: initial mean tumor size, k_a: TMZ absorption rate, V : TMZ volume of distribution, Cl: TMZ clearance, π_{PAR}: probability to belong to the cluster with acquired resistance, σ: residual error standard deviation.

Table 2: Multivariate survival analysis using Cox proportional hazard model.

	Hazard Ratio	95 % Confidence Interval	p-value
Acquired Resistance Cluster	3.65	1.65 – 8.1	0.00143
Age (year)	1.032	0.99 - 1.067	0.07
	1.018	0.997 - 1.0385	0.09
Tumor Size at TMZ Onset (mm)			
p53 overexpression	1.01	0.42 - 2.43	0.97
IDH Mutation	1.09	0.47 - 2.51	0.83
1p/19q Chromosomal Co-deletion	0.17	0.05 - 0.65	0.009

Figure 1

Observed tumor mean diameter in three patients. Dots represent observed mean tumor diameters. Gray shaded intervals correspond to TMZ administration.

Figure 2

Schematic representation of the two tumor growth inhibition models (left: model with primary resistance only, right: model with primary and acquired resistance). LGG cells are divided into cells sensitive to TMZ (S), cells damaged by TMZ (D), primary resistant cells (R_P), and acquired resistant cells produced by chemotherapy exposition (R_A). λ: division rate of sensitive and primary resistant cells, Δ_R: increase in division rate of acquired resistant cells, τ_{SD}: transition rate from sensitive to damaged cells, τ_{DR}: transition rate from damaged to acquired resistant cells, μ_D: death rate of damaged cells, k_S: proportion of sensitive cells at the beginning of the follow-up.

Figure 3

Observations versus model predictions (top: population predictions, bottom: individual predictions) for each cluster [left: cluster with primary and acquired resistance, middle: cluster with primary resistance only (TMZ treated patients), right: cluster with primary resistance only (PCV treated patients)].

Figure 4

Visual Predictive Check plots in both clusters for TMZ treated patients. Left: Median, 5% and 95% quantiles of model simulations for model PR, ie with primary resistance only. Dots represent individual data for patients clustered in PR profile. Right: Median, 5% and 95% quantiles of model simulations for model PAR, ie with primary and acquired resistant cells.

Dots represent individual data for patients clustered in PAR profile.

Figure 5

Evolution of individual mean tumor diameter simulations in 9 representative patients. Black dots correspond to mean tumor diameters. Black curves correspond to simulated mean tumor diameters. Green, yellow, light red and dark red curves respectively correspond to sensitive, damaged, acquired and primary resistant cells. First row: Patients with primary and acquired resistance treated with TMZ. Second row: Patients with primary resistance only treated with TMZ. Third row: Patients with primary resistance only treated with PCV.

Figure 6

Left and middle: comparison of clinical outcomes between patients with and without acquired resistance. Red curve corresponds to the group with primary and acquired resistant cells (PAR profile). Blue curve corresponds to the group with primary resistance only (PR profile). Black marks correspond to censored observations. Left: Kaplan-Meier estimates of progression free survival since treatment onset in patients with and without acquired resistance. Middle: Kaplan-Meier estimates of overall survival from treatment onset in both cluster. Right: Kaplan-Meier estimates of overall survival since treatment onset stratified according to 1p/19q chromosomal co-deletion status and resistance clusters for patients treated with TMZ. Red survival curve corresponds to the group with primary and acquired resistance without 1p/19q chromosomal co-deletion. Green survival curve corresponds to the group with primary and acquired resistance with 1p/19q chromosomal co-deletion. Purple survival curve corresponds to the group with primary resistance only with 1p/19q chromosomal co-deletion. Blue survival curve corresponds to the group with primary

resistance only without 1p/19q chromosomal co-deletion. Black marks correspond to censored observations.

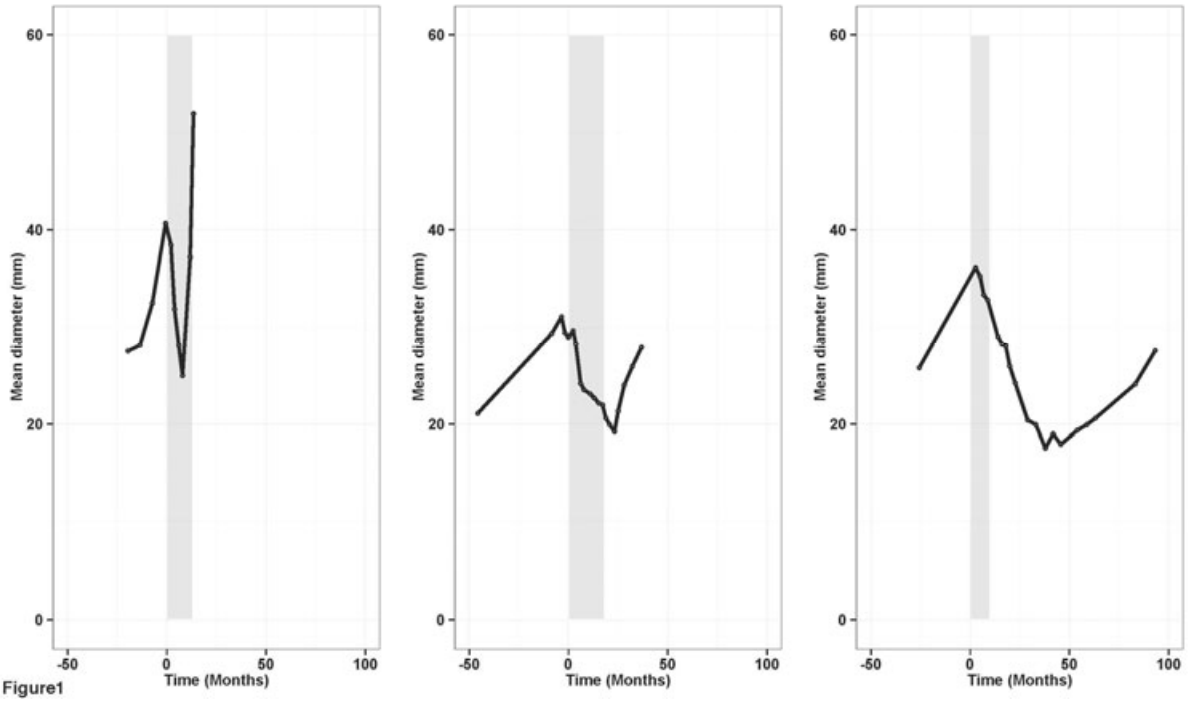

Figure1

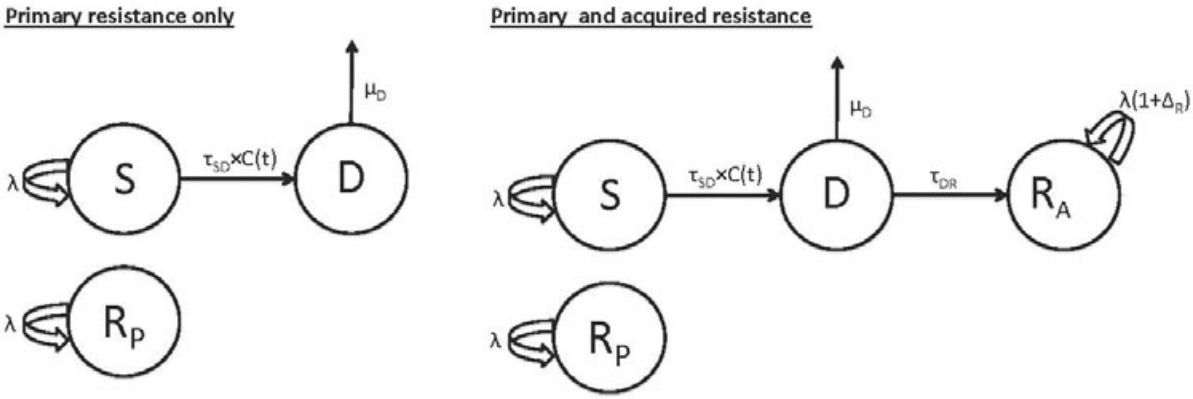

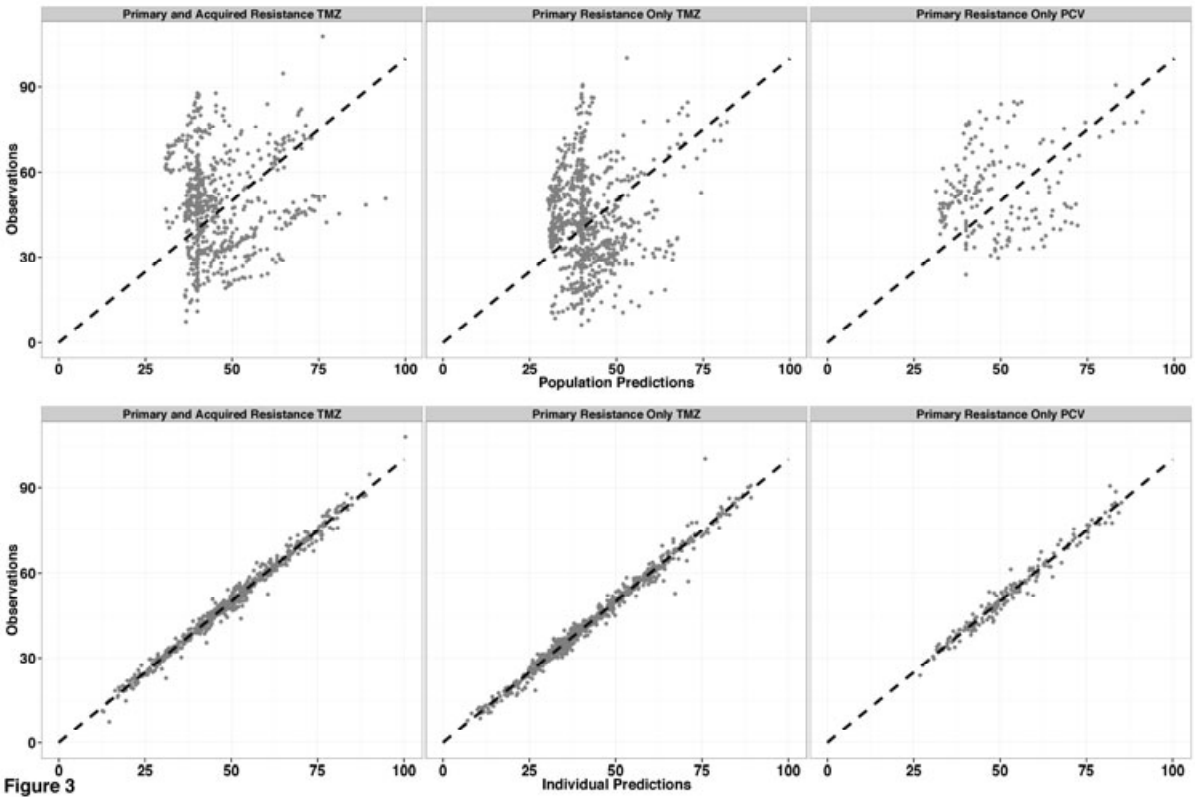

Figure 3